

Mixed-Valence Behavior in an Iodine Complex of a Ferrocenylenesilylene Polymer

K. H. Pannell,^{*,†} V. I. Imshennik,[‡] Yu. V. Maksimov,[‡] M. N. Il'ina,[§] H. K. Sharma,[†]
V. S. Papkov,^{*,§} and I. P. Suzdalev^{*,‡}

Department of Chemistry, The University of Texas at El Paso, El Paso, Texas 79968, Institute of Chemical Physics, Russian Academy of Sciences, Kosygin str. 4, 117334 Moscow, Russia, and Institute of Organoelement Compounds, Russian Academy of Sciences, Vavilov str. 28, 119991 Moscow, Russia

Received July 20, 2004

Structural and thermal characteristics of an amorphous iodine complex of a ferrocenylenesilylene polymer, $[-(\text{C}_5\text{H}_4)\text{Fe}(\text{C}_5\text{H}_4)\text{Si}(\text{CH}_3)(\text{C}_6\text{H}_5)(\text{I}_{1.5})-]_n$, have been measured using ^{57}Fe Mössbauer, IR and Raman spectroscopy, X-ray diffraction, and thermomechanical analysis. The iodine-doped macromolecules are mixed-valence salts with a localized electron structure on the ^{57}Fe Mössbauer time scale, in which ferrocenylene units and ferrocenium moieties coexist. These macromolecules consist of blocks containing ferrocenium moieties and sequences of nonoxidized ferrocenylene units. The environment about the ferrocenium moieties consists of both single I_3^- and polyiodide $[\text{I}_3]^- \cdot n\text{I}_2$ species. Mössbauer data, collected in the range 5–300 K, are interpreted in terms of the temperature dependence of the Lamb–Mössbauer factor and reversible electron transfer with an activation energy of 4.7 kJ/mol. The transformations of $[\text{I}_3]^- + \text{I}_2$ clusters to I_3^- are proposed to accompany $\text{Fe(II)}-\text{Fe(III)}$ oxidation.

Introduction

Considerable research attention has been focused on mixed-valence complexes due to their electrical and magnetic properties and the importance of mixed-valence biological systems.¹ For example, bisferrocenyl complexes exhibit valence delocalization on a variety of different time scales depending on the type of bridging groups between the ferrocenyl moieties, the substituents on the cyclopentadienyl rings, and the nature of the solid-state environment about the mixed-valence cation.² Recent advances in the synthesis of organometallic polymers containing metallocene moieties in the main polymer chain, or as pendant groups, offer the prospect of producing novel types of smart materials which combine specific properties of low molecular weight mixed-valence compounds with the various useful mechanical characteristics and processing advantages of polymers.^{3,4} We have a continuing interest in one type of such polymers, the

poly(ferrocenylenesilylenes) (PFOSs), whose main chains consist of alternating ferrocenylene and organosilylene units: $[-(\text{C}_5\text{H}_4)\text{Fe}(\text{C}_5\text{H}_4)\text{SiR}_2-]_n$, R = various alkyl or aryl groups.⁵ Such high molecular weight PFOSs can be obtained by thermal, transition-metal-catalyzed, or anionic ring-opening polymerization of the corresponding [1]-silylene-ferrocenophanes.^{5,6}

Cyclic voltammetric analysis of PFOS^{5a-c,6a,7} shows two reversible oxidation waves similar to those reported earlier for diferrocenylacetylene.⁸ Furthermore, the triiodide salt of the latter compound gave an example of electron transfer in mixed-valence ions.⁹ The two-step oxidation of PFOS was interpreted to be a result of the sequential oxidation of each

[†] The University of Texas at El Paso.

[‡] Institute of Chemical Physics, Russian Academy of Sciences.

[§] Institute of Organoelement Compounds, Russian Academy of Sciences.

- (1) (a) *Mixed-Valence Compounds, Theory and Applications in Chemistry, Physics, Geology and Biology*; Brown, D. W., Ed.; Reidel Publishing Co.: Boston, MA, 1980. (b) Creutz, C. *Prog. Inorg. Chem.* **1983**, *30*, 1. (c) *Mixed Valency Systems, Applications in Chemistry, Physics and Biology*; Prassides, K., Ed.; Kluwer Academic Publishers: Dordrecht, The Netherlands, 1991.
- (2) Selected references: (a) Hendrickson, D. N. In *Mixed Valency Systems, Applications in Chemistry, Physics and Biology*; Prassides, K., Ed.; Kluwer Academic Publishers: Dordrecht, The Netherlands, 1991; p 67. (b) Morrison, W. H., Jr.; Hendrickson, D. N. *Inorg. Chem.* **1975**, *14*, 2331. (c) Moore, M. F.; Wilson, S. R.; Cohn, M. J.; Dong T.-Y.; Mueller-Westerhoff, U. T.; Hendrickson, D. N. *Inorg. Chem.* **1985**, *24*, 4559. (d) Hendrickson, D. N.; Oh, S. M.; Dong, T.-Y.; Kambara, T.; Cohn, M. J.; Moore, M. F. *Comments Inorg. Chem.* **1985**, *4*, 329. (e) Dong T.-Y.; Hendrickson, D. N.; Pierpont, C. G.; Moore, M. F. *J. Am. Chem. Soc.* **1986**, *108*, 963. (f) Nakashima, S.; Nishimori, A.; Masuda, Y.; Sano, H.; Sorai, M. *J. Phys. Chem. Solids* **1991**, *52*, 1169. (g) Webb, R. J.; Hagen, P. M.; Wittebort, R. J.; Sorai, M.; Hendrickson, D. N. *Inorg. Chem.* **1992**, *31*, 1791 and references therein.
- (3) (a) *Inorganic and Organometallic Polymers II*; Wisian-Nielson, P., Allcock, H. R., Wynne, K. J., Eds.; ACS Symposium Series 572; American Chemical Society: Washington, DC, 1994. (b) *Metal Containing Polymer Systems*; Sheets, J. E., Carraher, C. E., Pittman, C. U., Eds.; Plenum: New York, 1985. (c) Nishihara, H. *Organometallic Conductive Polymers*. In *Handbook of Organic Conductive Molecules and Polymers*. 2. *Conductive Polymers: Synthesis and Electrical Properties*; Nalwa, H. S., Ed.; John Wiley & Sons: New York, 1997; p 799.
- (4) (a) Cowan, D. O.; Park, J.; Pittman, C. U., Jr.; Sasaki, Y.; Mukherjee, T. K.; Diamond, N. A. *J. Am. Chem. Soc.* **1972**, *94*, 5110. (b) Pittman, C. U., Jr.; Sasaki, Y. *Chem. Lett.* **1975**, 383. (c) Merz, A.; Bard, A. J. *J. Am. Chem. Soc.* **1978**, *100*, 3222. (d) Daum, P.; Murray, R. W. *J. Chem. Phys.* **1981**, *85*, 389. (e) Brandt, P. F.; Rauchfuss, T. B. *J. Am. Chem. Soc.* **1992**, *114*, 1926. (f) Rudzinski, W. E.; Walker, M.; Horwitz, C. P.; Suhu, N. Y. *Electroanal. Chem.* **1992**, *335*, 265. (g) Stanton, C. E.; Lee, T. R.; Grubbs, R. H.; Lewis, N. S. *Macromolecules* **1995**, *28*, 8713. (h) Buretea, M. A.; Tilley, T. D. *Organometallics* **1997**, *16*, 1507. (i) Deschenaux, R.; Jauslin, I.; Scholten, U.; Turpin, F. *Macromolecules* **1998**, *31*, 5647.
- (5) (a) Nguyen, M. T.; Diaz, A. F.; Dementiev, V. V.; Sharma, H. H.; Pannell, K. H. *SPIE Proc.* **1993**, *1910*, 230. (b) Nguyen, M. T.; Diaz, A. F.; Dementiev, V. V.; Pannell, K. H. *Chem. Mater.* **1993**, *5*, 1389. (c) Nguyen, M. T.; Diaz, A. F.; Dementiev, V. V.; Pannell, K. H. *Chem. Mater.* **1994**, *6*, 952. (d) Pannell, K. H.; Dementiev, V. V.; Li, H.; Cervantes-Lee, F.; Nguyen, M. T.; Diaz, A. F. *Organometallics* **1994**, *13*, 3644. (e) Papkov, V. S.; Gerasimov, M. V.; Dubovik, I. I.; Sharma, S.; Dementiev, V. V.; Pannell, K. H. *Macromolecules* **2000**, *33*, 7107.

of two neighbor iron atoms alternating along the main chain. Thus, oxidized PFOS macromolecules can in principle exist both as polycations bearing the positive charge on every iron center and as mixed-valence polycations with alternating ferrocenylene and ferrocenium units along the backbone, thereby affecting the optoelectrical and other properties of the oxidized polymer.

Iodine-doped thin PFOS films were reported to exhibit electroconductivity at a level of semiconductors,¹⁰ like a variety of iodine-doped organic polymers containing ferrocenyl units.^{3c,4a,b} These materials can be related to so-called conductive low-dimensional halogenated systems whose electrical properties are controlled by the level of oxidation and by the type of $[I]^{-} \cdot nI_2$ anions formed and their mutual packing.¹¹ A linear ferrocenylenedimethylsilylene oligomer containing seven repeat units was readily oxidized by I_2 to yield a crystalline complex with alternating Fe^{2+} and Fe^{3+} centers, with concurrent formation of I_3^{-} anions.⁷ Similarly, the iodide complex of 1,1'-bis(trimethylsilyl)ferrocene, $[(\eta^5-Me_3SiC_5H_4)_2Fe]$, contains I_3^{-} species as counteranions.^{10e} However, contrary to these crystalline low molecular weight complexes, we reported that semicrystalline and amorphous iodine-doped high molecular weight poly(ferrocenylenesilylenes) contained higher polyiodide anions, e.g., I_5^{-} as well as $[I_3]^{-}$.^{10e} Furthermore, we proposed that these higher polyiodide anions are formed in amorphous regions of the polymers and also demonstrated that the transformation of $[I_3]^{-} \rightarrow [I_5]^{-}$ ($I_3^{-} \cdot I_2$) significantly affected the polymer conductivity.

Given these results, insight into the structure of the oxidized moieties in iodide PFOS complexes in different phase states is of special interest. We now describe some structural and thermal characteristics of an amorphous iodine complex of poly(ferrocenylenemethylphenylsilylene), $[-(C_5H_4)Fe(C_5H_4)Si(CH_3)(C_6H_5)-]_n$, (MePh-PFOS), with an emphasis on the valence state of the iron atoms as revealed by means of ^{57}Fe Mössbauer spectroscopy in the temperature range 5–300 K.

Experimental Section

Materials. MePh-PFOS was prepared as previously reported;^{5a,b} GPC analysis of the specific sample in THF indicated $M_w = 295000$ and $M_n = 100500$ (referenced to a polystyrene calibration curve).

- (6) (a) Foucher, D. A.; Tang, B.-Z.; Manners, I. J. *J. Am. Chem. Soc.* **1992**, *114*, 6246. (b) Rulkens, R.; Ni, Y.; Manners, I. *J. Am. Chem. Soc.* **1994**, *116*, 12121. (c) Rulkens, R.; Lough, J. K.; Manners, I. *J. Am. Chem. Soc.* **1994**, *116*, 797. (d) Ni, Y.; Rulkens, R.; Pudelski, J. K.; Manners, I. *Macromol. Rapid Commun.* **1995**, *16*, 637. (e) Gomez-Elipe, P.; Macdonald, J.; Manners, I. *J. Angew. Chem., Int. Ed. Engl.* **1997**, *36*, 762.
- (7) Rulkens, R.; Lough, A. J.; Manners, I.; Lovelace, S. R.; Grant, C.; Geiger, W. E. *J. Am. Chem. Soc.* **1996**, *118*, 12683.
- (8) LeVanda, C.; Cowan, D. O.; Leitch, C.; Bechgaard, K. *J. Am. Chem. Soc.* **1974**, *96*, 6788.
- (9) Kramer, J. A.; Hendrickson, D. N. *Inorg. Chem.* **1980**, *19*, 3330.
- (10) (a) Tanaka, M.; Hayashi, T. *Bull. Chem. Soc. Jpn.* **1993**, *66*, 334. (b) Manners, I. *Adv. Organomet. Chem.* **1995**, *16*, 637. (c) Rulkens, R.; Resendes, R.; Manners, I.; Murti, K.; Fossum, E.; Miller, P.; Matyjaszewski, K. *Macromolecules* **1997**, *30*, 8165. (d) Bakueva, L.; Sargent, E. H.; Resendes, R.; Bartole, A.; Manners, I. *Mater. Sci.: Mater. Electron.* **2001**, *12*, 21. (e) Espada, L.; Shadaram, M.; Pannell, K. H.; Papkov, V. S.; Leites, L. A.; Bukalov, S. S.; Tanaka, M.; Hayashi, T. *Organometallics* **2002**, *21*, 3758.
- (11) Marks, T. J.; Kalina, D. W. in *Extended Linear Chain Compounds*; Miller, J. S., Ed.; Plenum: New York, 1982; pp 1 and 197.

Synthesis of an Iodine + MePh-PFOS Complex. Samples of the iodine complex were prepared by rapid mixing of a 1.5 wt % benzene solution of MePh-PFOS with a 1.5 wt % solution of I_2 with vigorous stirring (molar ratio I_2 :repeat unit = 1:1). Upon mixing, a very viscous liquid phase of an iodine complex separated from the solution, which gradually precipitated. The reaction mixture was allowed to settle for several days to achieve a more complete phase separation. The upper benzene layer was decanted, and after additional washing with benzene the complex was first dried in air and subsequently in a vacuum at 40–50 °C. The dried residue was mildly ground to produce a powder whose smallest particles observed under a microscope had a dark brown color. Elemental analysis of the dried complex: C, 42.0; H, 3.50; Fe, 12.4; I, 38.6.

Thermomechanical analysis (TMA) was carried out using a UIP-70M (USSR) thermomechanical analyzer permitting measurement of the strain with an accuracy of 0.001 mm. MePh-PFOS and its iodine complex samples of about 1 mm thick (powders compressed under a pressure of 5.0 MPa at ambient temperature) were placed in a steel cup (6 mm inner diameter). The diameter of a cylindrical indenter with the flat end connected to a measuring quartz probe was 2.52 mm. Thermomechanical traces (penetration of the indenter vs temperature) were recorded at a heating rate of 5 °C/min under dead load (0.1 MPa).

Thermogravimetric analysis (TGA) was performed on a UVDT-500 (USSR) thermogravimetric analyzer in a vacuum (2×10^{-3} Torr) and in an atmosphere of argon at a heating rate of 5 °C/min using samples of 0.8–0.9 mg by weight. X-ray diffractograms were taken on a DRON-3 (Russia) diffractometer in reflection mode with the use of nickel-filtered Cu K α radiation. Raman spectra were recorded with a Ramanor HG-2S laser spectrometer using the 514.5 nm line from an ILA-120 argon laser. IR spectra were recorded by means of an IR Specord 82. Mössbauer measurements were performed on a conventional Mössbauer spectrometer with a 1.13 GBq ^{57}Co (Rh) source maintained at room temperature. The absorber temperature was varied in the range 5–300 K by means of an Oxford Instrument cryostat. Isomer shifts are reported relative to the peak for α -Fe at room temperature.

Result and Discussion

General Characterization of Iodide Polymer Salt. The two-step electrochemical oxidation of PFOS initially leading to the more thermodynamically stable alternating ferrocenylenylene and ferrocenium polymer backbone^{5a–c,6a,7} suggests that one could expect the formation of such a structure under controlled mild conditions of oxidation of PFOS with I_2 . Treatment of a dilute solution of MePh-PFOS with a small excess of I_2 led to a material whose elemental analysis exhibited ~39 wt % iodine, which corresponds to the “expected” 1.5 I atoms per monomer repeat unit. The IR spectrum of this complex, Figure 1, exhibits bands at 833 and 862 cm^{-1} of almost equal intensities that can be associated with an out-of-plane CH bending in ferrocenylenylene and ferrocenium moieties, respectively.^{7,9} However, its Raman spectrum, Figure 2, exhibits two bands at 109 cm^{-1} ($[I_3]^{-}$)^{11,12} and ~170 cm^{-1} ($[I_5]^{-}$).^{11,13} Thus, less than half

- (12) (a) Teitebaum, R. C.; Ruby, S. L.; Marks, T. J. *J. Am. Chem. Soc.* **1980**, *102*, 3322. (b) Deplano, P.; Devillanova, F. A.; Ferraro, J. R.; Isaia, F.; Lippolis, V.; Mercuri, M. L. *Appl. Spectrosc.* **1992**, *46*, 1625. (c) Nour, E. M.; Shahada, L. *Spectrochim. Acta* **1989**, *45A*, 1033.
- (13) (a) Parrett, F. W.; Taylor, N. J. *J. Inorg. Nucl. Chem.* **1969**, *32*, 2458. (b) Milne, J. *Spectrochim. Acta* **1992**, *48A*, 533.

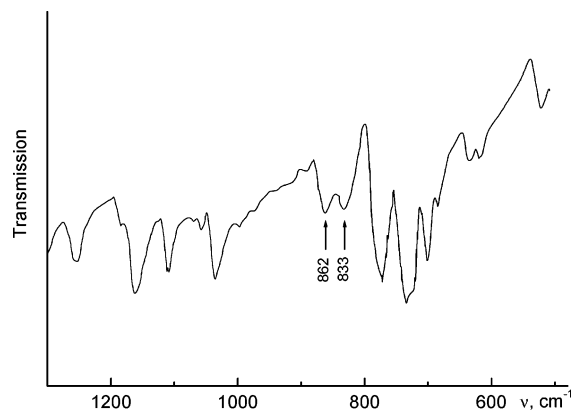


Figure 1. IR spectrum of iodine-doped poly(ferrocenylenemethylphenylsilylene).

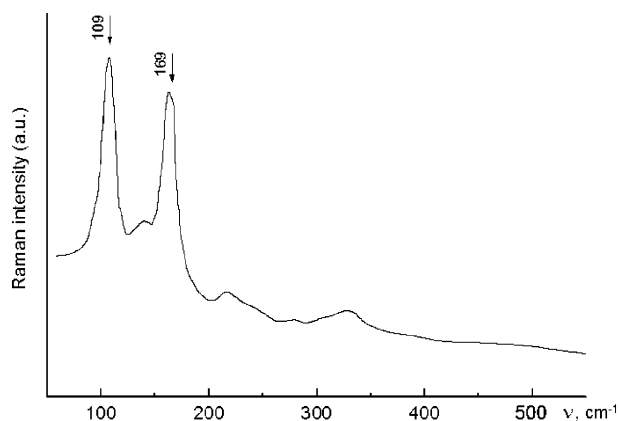


Figure 2. Raman spectrum of iodine-doped poly(ferrocenylenemethylphenylsilylene).

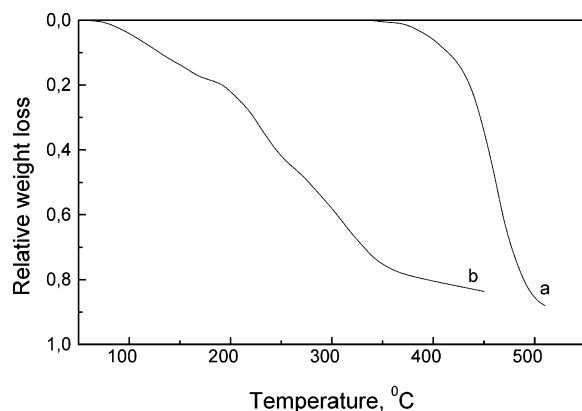


Figure 3. TGA curves for poly(ferrocenylenemethylphenylsilylene) (a) and its iodide complex (b) taken in a vacuum (10^{-3} Torr) at a heating rate of $5\text{ }^{\circ}\text{C}/\text{min}$.

of the ferrocenylene moieties were oxidized, and the expected uniform structure with alternating ferrocenylene and ferrocenium moieties could not be possible.

Formation of the polyiodide anions higher than $[\text{I}_3]^-$, i.e., $[\text{I}_3]^- \cdot n\text{I}_2$, is also evidenced by the fact that $\sim 25\%$ of the iodine atoms in this complex can be removed by exposure to high vacuum. After this loss of iodine the stability of the resulting complex was studied by TGA measurements carried out in a vacuum and under an atmosphere of argon, Figure 3. Both conditions produced the same data, suggesting that the weight loss is not controlled by diffusion. The TGA curve reflects a three-stage loss of weight upon heating in which both the first and second stages are mainly connected with

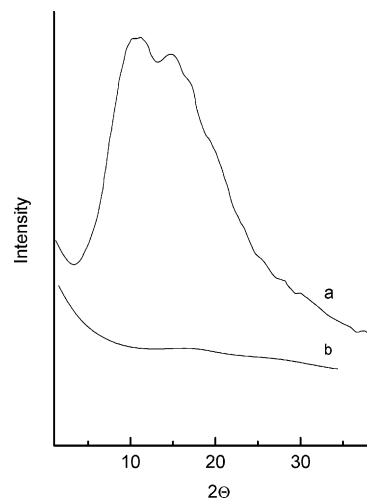


Figure 4. X-ray diffractograms for poly(ferrocenylenemethylphenylsilylene) (a) and its iodide complex (b). Nickel-filtered $\text{Cu K}\alpha$ radiation, $\lambda = 0.1542\text{ nm}$.

the I_2 elimination. In the first stage removal of I_2 is accompanied initially by only a decrease in intensity of the 170 cm^{-1} band in the Raman spectra, while the IR spectra in the region $800\text{--}900\text{ cm}^{-1}$ remain practically unchanged. This is similar to the behavior observed upon extended pumping of iodine-doped films of MePh-PFOS.^{10e} Upon further heating the intensity of the 862 cm^{-1} band in the IR spectra also diminished, indicating a gradual decrease in the content of $[\text{I}_5]^-$ followed by a similar decrease in the $[\text{I}_3]^-$ content with rising temperature. Significant destruction of the remaining partially oxidized macromolecules begins at $\sim 220\text{ }^{\circ}\text{C}$, i.e., about $110\text{ }^{\circ}\text{C}$ lower than that of the neat MePh-PFOS.

An X-ray diffraction study showed that the initially formed iodine complex is amorphous like the undoped polymer, Figure 4. However, the X-ray diffractograms of the two materials are quite different. The X-ray diffractogram for MePh-PFOS contains two rather sharp amorphous halos superimposed on each the other and centered at the diffraction angles $2\theta \cong 12.5^{\circ}$ and 16.8° . The former appears to arise from a short-range order in the direction perpendicular to the main chain axis. The iodine polymer complex displays only diffusive X-ray scattering. Such a drastic change in the diffraction curve profile after iodine doping can be explained by a strong absorption of X-rays by heavy iodine atoms and the absence of a short-distance periodicity in the electron density in the regions containing polyiodide anions. Furthermore, no periodicity on a scale up to 100 nm was found in the complex using small-angle X-ray scattering.

The iodide polymer complex, which was initially separated from a benzene solution as a very viscous phase (see the Experimental Section), failed to swell in benzene after drying. Nevertheless, it could soften and then flow upon heating as noted from the TMA trace shown in Figure 5. The glass transition (softening) temperature of the complex determined as a penetration onset temperature ($\sim 50\text{ }^{\circ}\text{C}$) proved to be lower than that for the pristine polymer ($\sim 90\text{ }^{\circ}\text{C}$). This seems to be a counterintuitive and surprising observation since the formation of ionic links between ferrocenium units and iodide counteranions is expected to confer a higher rigidity upon the macromolecule salts. However, it can be noted that the

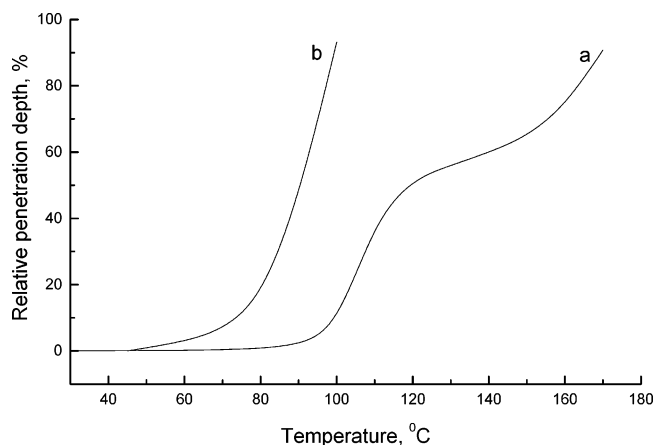


Figure 5. Thermomechanical traces for poly(ferrocenylmethylphenylsilylene) (a) and its iodide complex (b). Load 0.1 MPa, heating rate 5 °C/min.

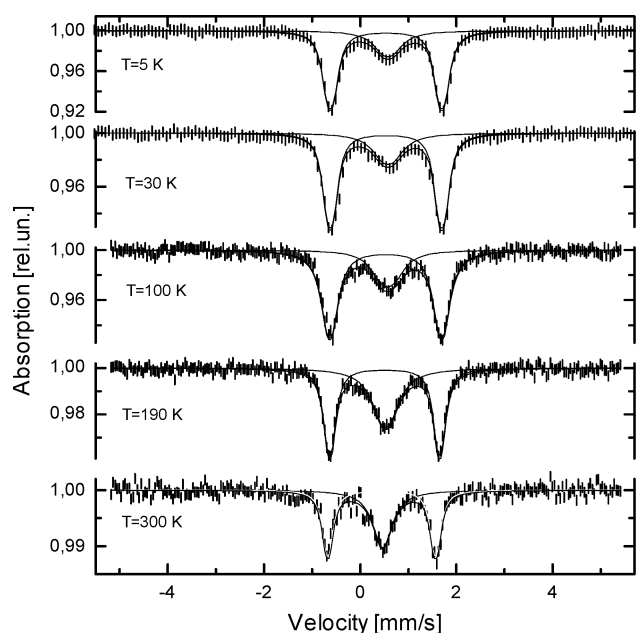


Figure 6. ^{57}Fe Mössbauer spectra for the iodide complex of poly(ferrocenylmethylphenylsilylene) at various temperatures.

softening of the complex occurs concurrently with the onset of iodine loss, and we suggest that a plasticizing effect of the released iodine molecules is responsible for this observation. Another reason could be scission of the original macromolecules due to destructive side reactions upon oxidizing of ferrocenylene units by I_2 .

^{57}Fe Mössbauer Spectra. Figure 6 shows the evolution of ^{57}Fe Mössbauer spectra over the temperature range of 5–300 K. The resulting spectra were fitted by an outer doublet and an inner singlet. Their spectral fitting parameters (isomer shifts δ_1 and δ_2 , quadrupole splitting ΔE_{Q1} , line widths Γ_1 and Γ_2 , respectively) at various temperatures are given in Table 1. Mössbauer spectral variations with temperature are reversible, and the Mössbauer spectra of the nondoped pristine polymer consist at all temperatures only of doublets with parameters similar to those observed for the outer doublets of the iodide complex.

The evaluated doublet and singlet parameters are in agreement with those reported for Fe(II) atoms in ferrocene and its derivatives,¹⁴ and for Fe(III)⁺ cation in ferrocenium

Table 1. Mössbauer Parameters for Fe(III)⁺ and Fe(II) Species in Ferrocenium and Ferrocene Moieties of the Iodine Complex of Poly(ferrocenylmethylphenylsilylene) at Various Temperatures^a

temp, K	Fe species	δ , mm/s (± 0.03)	ΔE_{Q} , mm/s (± 0.03)	Γ , mm/s (± 0.03)
5	Fe(III) ⁺	0.80		0.65
	Fe(II)	0.75	2.30	0.28
30	Fe(III) ⁺	0.77		0.60
	Fe(II)	0.75	2.30	0.29
100	Fe(III) ⁺	0.58		0.70
	Fe(II)	0.53	2.29	0.37
190	Fe(III) ⁺	0.52		0.61
	Fe(II)	0.50	2.27	0.26
300	Fe(III) ⁺	0.47		0.49
	Fe(II)	0.45	2.27	0.24

^a δ , relative to the peak for $\alpha\text{-Fe}$; ΔE_{Q} , quadrupole splitting; Γ , line width.

bromide,¹⁵ triiodide salts of ferrocenium, and dioxidized cation *exo,exo*-1,12-dimethyl[1.1]ferrocenophanium.^{2c} The parameters are similar to those from earlier analyses of mixed-oxidation state ferrocenyl-containing polymers.¹⁶ Thus, in the iodine-doped polymer a complex structure of ferrocenylene and ferrocenium units exists as a mixed-valence polycation with a localized electron structure on the ^{57}Fe Mössbauer time scale; i.e., the rate of intramolecular electron transfer is less than $\sim 10^7 \text{ s}^{-1}$. Similar localized mixed-valence triiodide salts are formed by some biferrocenes with hydrocarbon bridges between the ferrocenyl groups. On the other hand, salts of various biferrocenes with directly connected ferrocenyl nuclei exhibit delocalized mixed-valence behavior.²

The inner singlet in the spectra is in fact an unresolved doublet. It can be least-squares fitted by Lorentzian line shapes with a very small quadrupole splitting ΔE_{Q2} (~ 0.2 , 0.3 , and 0.15 mm s^{-1} at 77, 130, and 300 K, respectively) and equal intensities and line widths of the components. Note that no magnetic (paramagnetic) hyperfine splitting of the ferrocenium singlet is observed in the spectrum taken at 5 K, and this fact points to a fast spin relaxation for Fe(III) spin with a rate greater than 10^{10} s^{-1} . Such a fast spin relaxation is apparently generated by spin–spin relaxation, which becomes possible due to a rather short distance between neighboring iron atoms in the polymer main chain ($\sim 6.9 \text{ \AA}$), and also by a fast spin–lattice relaxation, which proceeds owing to a large orbital moment input in the total atomic moment of Fe^{3+} .¹⁷

The temperature dependencies of the normalized doublet and singlet areas, S_1 and S_2 , respectively, are shown in Figure 7a. Both plots can be divided schematically into two sections: a low-temperature region with practically constant values of S (extended over ~ 5 –50 K for S_1 and over ~ 5 –140 K for S_2) and a high-temperature region where the plots

- (14) Herber, R. H.; Kingston, W. R.; Wertheim, G. K. *Inorg. Chem.* **1963**, *2*, 153.
- (15) (a) Wertheim, G. K.; Herber, R. H. *J. Chem. Phys.* **1963**, *38*, 2106. (b) Lesikar, A. V. *J. Chem. Phys.* **1964**, *40*, 2746.
- (16) (a) Pittman, C. U., Jr.; Lai, J. C.; Vanderpool, D. P.; Good, M.; Prados, R. *Macromolecules* **1970**, *3*, 746. (b) Pittman, C. U., Jr.; Lai, J. C.; Vanderpool, D. P.; Good, M.; Prados, R. In *Polymer Characterization: Interdisciplinary Approaches*; Carver, C. D., Ed.; Plenum Press: New York, 1971; p 97.
- (17) (a) Suzdalev, I. P. *Dynamic effects in gamma-resonance spectroscopy*; Atomizdat: Moscow, 1979. (b) Suzdalev, I. P.; Kurinov, I. V.; Tsybmal, E. Yu.; Matveev, V. V. *J. Phys. Chem. Solids* **1994**, *55*, 127.

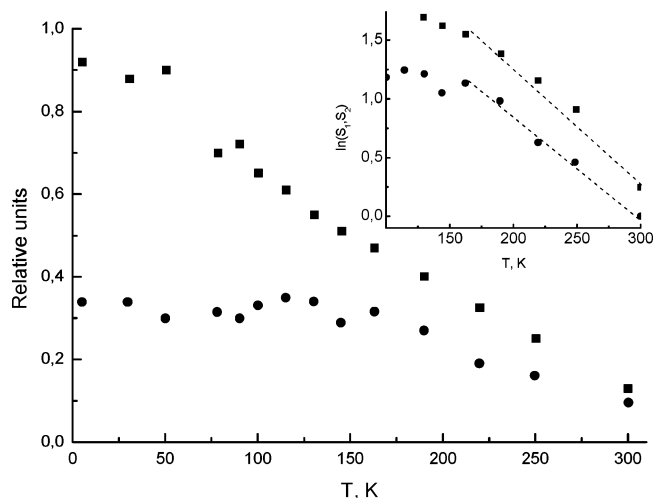


Figure 7. Normalized spectral areas S_1 of ferrocene units (■) and S_2 of ferrocenium units (●) as functions of temperature. Inset: $\ln(S_1, S_2)$ as a function of temperature.

can be approximated by straight lines with different slopes. The different temperature dependencies of S_1 and S_2 mean that the relative singlet spectral area $S_2^R = S_2/(S_1 + S_2)$, which can be used for estimating the ferrocenium unit content in the iodine-doped polymer, changes with increasing temperature. The temperature dependence of S_2^R is shown in Figure 8. At temperatures from 5 to 50 K the value of S_2^R is practically constant and equal to ~ 0.25 , and then, in the temperature range 50–115 K, it increases to ~ 0.37 and continues to grow slowly up to ~ 0.47 at 300 K. The variation of S_1 , S_2 , and S_2^R with temperature is an important observation and requires some detailed explanation.

For a fine absorber of γ -rays the spectral area S is

$$S \cong f_s n_a f_a \sigma_a \quad (1)$$

where f_s is the free recoil fraction of the source, n_a and σ_a represent the number of resonant ^{57}Fe atoms and resonance cross-section in the absorber, respectively, and $f_a = \exp(-2W)$ is the Lamb–Mössbauer factor, which determines the Mössbauer effect probability.^{17a,18} In the Debye approximation

$$2W = 6E_R T/k\Theta_D^2 \quad (2)$$

where E_R stands for the recoil energy of the ^{57}Fe atom, Θ_D is the Debye temperature of the moieties containing Fe atoms, and k is the Boltzmann constant. This approximation is valid at temperatures sufficiently higher than Θ_D .

In our analysis, we used the Debye approximation assuming the ferrocenylene and ferrocenium moieties to be segregated into two separate phases that do not affect one another. This is a simplified structural model of the of iodine-doped PFMPs, which is probably a very complex heterogeneous system where the oxidized and nonoxidized monomer units can be distributed along the main chains in various ways and aggregate into microdomains of different types interacting with each other. However, to date no proper

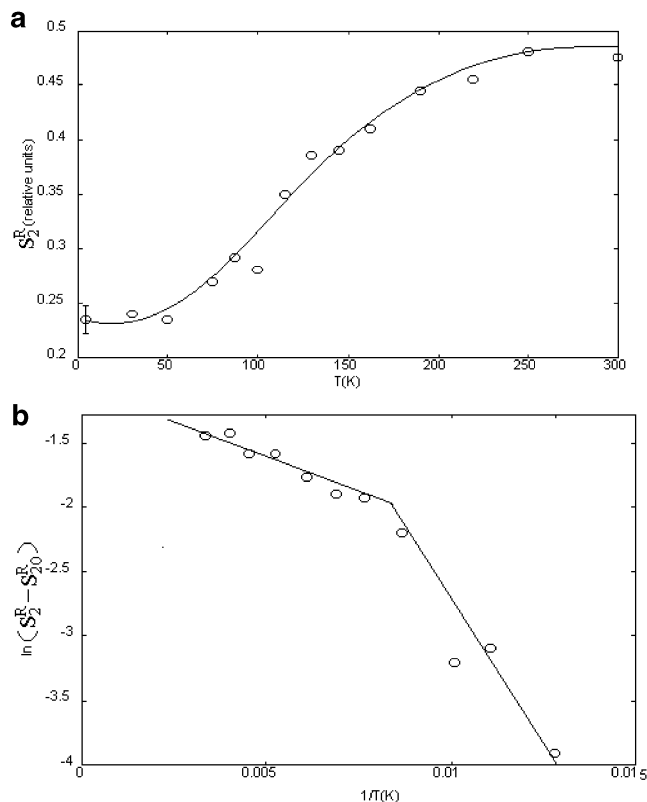


Figure 8. Relative ferrocenium unit spectral area $S_2^R = [S_2/(S_1 + S_2)]$ as a function of temperature (a) and its Arrhenius plot (b).

theoretical description of such heterogeneous systems has been developed.

According to eqs 1 and 2, the temperature variations of S_1 and S_2 should inversely depend on the square of the Debye temperatures of the ferrocenylene and ferrocenium moieties, Θ_{D1} and Θ_{D2} , respectively. As shown in Figure 7b the plots of $\ln S_1$ and $\ln S_2$ vs T are not linear over the whole temperature range, but their high-temperature sections between 190 and 300 K can be approximated by two straight lines. Their respective slopes of $\Theta_{D1} = 115$ K and $\Theta_{D2} = 122$ K reflect, in principle, a somewhat stronger interaction of the ferrocenium moieties with the iodine environment than the ferrocene moieties. The gently sloping high-temperature section of the S-shaped change of S_2^R with temperature, Figure 8, is in line with the difference between the calculated Debye temperatures.

At the same time, such a small difference between Θ_{D1} and Θ_{D2} cannot explain the steep upturn on the curve in the low-temperature range from 80 to 140 K. Other factors should determine this effect, including a particular pattern of the temperature dependence of the Lamb–Mössbauer factor f_a , resulting in the approximately constant value of S_2 over the relatively wide temperature interval while S_1 is markedly changing. It is difficult to specify the factors that can cause this type of temperature dependence of f_a .

According to eq 1, another parameter that can control the temperature dependence of S_1 and S_2 is the number of resonant $^{57}\text{Fe(III)}$ and $^{57}\text{Fe(II)}$ atoms. Thus, it seems possible to relate the sharp change in S_2^R with temperature to a temperature-dependent change in the number of Fe(III)^+ and Fe(II) centers. This suggestion implies that upon heating and cooling a certain fraction of Fe atoms can exhibit a reversible

(18) *Chemical Application of Mössbauer Spectroscopy*; Goldansky, V. I., Herber, R. H., Eds.; Academic Press: New York, London, 1968.

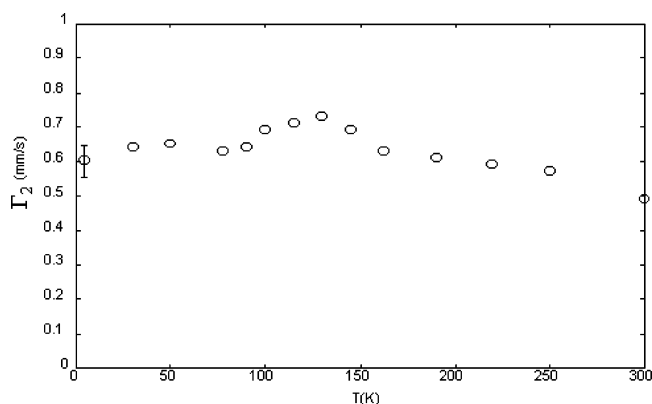


Figure 9. Line width of ferrocenium singlet Γ_2 in ^{57}Fe Mössbauer spectra as a function of temperature.

electron transition, $\text{Fe(II)} \rightleftharpoons \text{Fe(III)}$, resulting in the corresponding changes of S_2^R . A similar observation was suggested in conjunction with variable-temperature studies on mixed-valence poly(ferrocenylenedimethylvinylene) and copolymers of vinylferrocene with methylacrylate and with butylacrylate.¹⁹

We suggest that the proposed electron transition is a thermally activated electron hopping which can be described to a first approximation by

$$S_2^R = S_{20}^R + A \exp(-\Delta E_a/kT) \quad (3)$$

where S_{20}^R presents the initial S_2^R in the vicinity of 5 K, ΔE_a is the activation energy of electron hopping, and A is a constant. An Arrhenius plot of $\ln(S_2^R - S_{20}^R)$ versus reciprocal temperature, Figure 8b, gives two straight lines with the slopes corresponding to activation energies of 4.7 kJ/mol (0.043 eV) and ~ 0.7 kJ/mol in the temperature ranges 80–120 and 120–300 K, respectively. The latter magnitude of ΔE_a is too small to be connected with any electron-hopping process, and therefore, the observed slow increase of S_2^R at elevated temperatures should mainly be attributed to the different temperature dependence of the Lamb–Mössbauer factor in eq 1 due to different Debye temperatures for ferrocenylene and ferrocenium moieties. Note that the estimated value of the electron-hopping activation energy is of the same order of magnitude as the gap between the valence and electron conductivity bands observed for semiconductors with a defect or impurity mechanism of conductivity. This fact can in principle explain the electroconductivity reported for various PFOSs doped with iodine.

Considering possible reasons for the $\text{Fe(II)} \rightleftharpoons \text{Fe(III)}$ transition, it is expedient to note the occurrence of a small maximum in the temperature dependence of the spectral line width Γ_2 for $^{57}\text{Fe(III)}$ atoms. As shown in Figure 9, this maximum is centered at about 130 K and starts in the temperature region where the electron transition begins. Since the iodine polymer complex is of a trapped mixed-valence type on the Mössbauer time scale, the appearance of the Γ_2 maximum can apparently be explained by a structural

rearrangement in the iodine environment about the $^{57}\text{Fe(III)}$ species. This rearrangement seems to underlie the observed increase of quadrupole splitting ΔE_{Q2} from $\sim 0.2 \text{ mm s}^{-1}$ at 77 K to 0.3 mm s^{-1} at 130 K due to an increase in the crystal field gradient on the ^{57}Fe nuclei. Thus, the structural rearrangement facilitates the electron-hopping $\text{Fe(II)} \rightarrow \text{Fe(III)}$, resulting in the extra ferrocenium units in the iodine-doped macromolecules.

Complex Structure. It is not possible to depict in detail the structure of the iodide polymer salt nor the precise nature of the structural rearrangement proposed. However, a simplified model can be suggested on the basis of the above considerations. As noted in the preceding section, the iodine-doped macromolecules do not have the uniform structure of alternating ferrocenylene and ferrocenium moieties with the simplest $[\text{I}_3]^-$ counteranion despite the quantifiable presence of 1.5 iodine atoms for each repeat unit. The Mössbauer measurements showed that in the vicinity of 5 K only about one-quarter of the iron atoms are oxidized; i.e., on average there are six iodine atoms per ferrocenium unit. Therefore, in the low-temperature region, the environment about each ferrocenium moiety consists of an I_3^- anion associated with additional iodine atoms, thereby forming the polyiodide species similar to those reported for the well-known iodide complexes of low molecular weight organic compounds.¹¹ Above 50 K the fraction of Fe(III)^+ species increases due to the electron transition to a value of about 0.4 in the vicinity of 120 K. This value corresponds on average to ~ 4 iodine atoms per ferrocenium unit (or more specifically both an I_3^- and an I_5^- anion per pair of ferrocenium units). The coexistence of I_3^- and I_5^- anions in the iodine-doped polymer at room temperature is evidenced by the Raman spectra (Figure 2) discussed above. Thus, with increasing temperature iodine atoms from polyanions $\text{I}_3^- \cdot n\text{I}_2$ must be involved in the oxidation of extra ferrocenylene units with concurrent formation of the corresponding additional amount of I_3^- ions. To visualize how this process might proceed, it is necessary to have an idea of how the ferrocenium units distribute along the macromolecule.

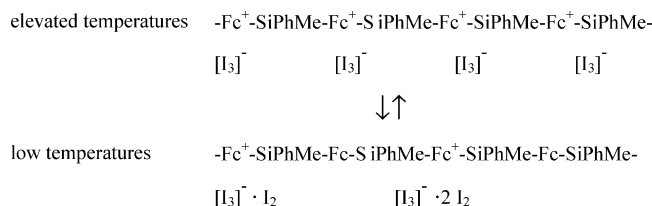
Two types of distribution can be proposed. The first involves a random distribution of ferrocenium units, i.e., an average structure of all polycation molecules. The second is a nonuniform multiblock structure of each polycation macromolecule, consisting of blocks of oxidized repeat units and sequences of nonoxidized ferrocenylene moieties. The different Debye temperatures Θ_{D1} and Θ_{D2} for ferrocenylene and ferrocenium moieties suggest the second heterogeneous structure of the iodide polymer complex, where the ferrocenylene and ferrocenium sequences can be aggregated into separated microdomains/clusters. However, our SAXS study has revealed no proper periodicity in the doped polymer, and hence, such microdomains are expected to have a very wide size distribution and diffusive interfaces.

Specifying the location of ferrocenium units within the oxidized sequences of the PFOS polymers is difficult. It is possible to assume that, upon doping, uncontrolled oxidation results in the formation of heterogeneous multiblock units, mainly due to strong adsorption of iodine from the solution into units of partially oxidized blocks with alternating

(19) (a) Wagener, W.; Hillberg, M.; Feyerherm, R.; Stieler, W.; Litterst, F. J.; Pohlmann, Th.; Nuyken, O. *J. Phys.: Condens. Matter* **1994**, *6*, L391. (b) Hillberg, M.; Stieler, W.; Litterst, F. J.; Bukhardt, V.; Nuyken, O. *Hyperfine Interact.* **1994**, *88*, 137.

ferrocenylene and ferrocenium moieties. This leads in turn to the occurrence of a second stage of oxidation, yielding the all-ferrocenium blocks. Such a structure of the oxidized blocks is expected to exist at elevated temperatures and to be retained upon cooling to the temperature range where the electron transition occurs. Such a conclusion is in accord with an earlier report that oxidation of some low molecular weight compounds and polymers containing ferrocenyl moieties with substoichiometric amounts of 2,3-dichloro-5,6-dicyanoquinone led to oxidized products with unexpectedly high Fe(III):Fe(II) ratios.²⁰

The electron transition at 140–80 K proceeds as an electron transfer from $[I_3]^-$ anions to $Fe(III)^+$ species, which is accompanied by a release of iodine atoms and the formation of larger $[I_3]^- \cdot nI_2$ counterions to neighboring ferrocenium moieties. In the course of this transition most of the all-ferrocenium sequences transform into sequences with alternating ferrocenylene and ferrocenium moieties, and consequently, the total amount of the ferrocenylene repeat units increases. Schematically this process can be presented as



The driving force of this process should be determined by differences in the free energies between the two types of

oxidized blocks and between the I_3^- and $I_3^- \cdot nI_2$ counteranions. Conversely, upon heating from liquid helium temperature the electron transition leads to the reverse electron hopping and the reestablishment of the all-ferrocenium sequences. As suggested above, the electron transition is connected with a certain structural transition in the doped MePh-PFOS. As the latter occurs at very low temperatures it is unlikely that it is due to large spatial rearrangements in the environment about the ferrocenium moieties. Rather, it could be associated with a specific temperature dependence of anharmonic vibrational modes in the iodide macromolecular complex. In this respect, it is pertinent to relate this transition to the “valence delocalization”, i.e., a transition from the localized electronic structure to the completely delocalized one. Such structures have been observed in some crystalline biferrocenium salts that occur due to the onset of anion vibrational motions, resulting in the triiodide ions interconverting between two configurations $I_A^- \cdots I_B-I_C$ and $I_A-I_B \cdots I_C^-$.^{2d-g} In our case, a more dramatic structural change involving the larger $[I_3]^- \cdot nI_2$ anions in the amorphous iodide complex seems to lead to more dramatic changes in their structure which result in the complete electron transfer and the transformation illustrated in the above scheme. Further investigation using low-temperature Raman/¹²⁹I Mössbauer spectroscopy is needed for verification of the above conclusions.

Acknowledgment. This research was supported by the Civilian Research Development Fund (CRDF) for collaborative research between the U.S. and former Soviet Union countries (Grant No. RC1-278) and the Welch Foundation, Houston, TX (Grant No. AH-0546). We thank Dr. L. A. Leites and Dr. S. S. Bukalov for the Raman spectra.

CM0403558

(20) Pittman, C. U., Jr.; Sasaki, Y.; Wilemon, G. *Tetrahedron Lett.* **1973**, 4399.